TECHNICAL NOTE

VOL. 43 | NO. 1 | **JANUARY - APRIL 2022** | PP 52-64

Revista Mexicana de Ingeniería Biomédica

dx.doi.org/10.17488/RMIB.43.1.5

E-LOCATION ID: 1214

Biomechanics Assessment of Kinematic Parameters of Low-Sprint Start in High-Performance Athletes Using Three Dimensional Motion Capture System

Mirvana Elizabeth Gonzalez Macias[1], *Carlos Villa Angulo*[2], *Emilio Manuel Arrayales Millan*[1], *Karla Raquel Keys Gonzalez*[1]

[1]Laboratory Biomechanics, Faculty of Sports, Autonomous University of Baja California, Mexicali, B. C., México

[2]Laboratory of Bioinformatics and Biofotonics, Engineering Institute, Autonomous University of Baja California, Mexicali, B. C., México

ABSTRACT

In a sprint start, the athlete takes up a position with their hands just behind a line, arms vertical, feet generally placed about a shoe length apart, and the hips rising above the line of the head. Mistakes in this position influence the execution of the low-sprint start, and can drastically influence the initial running speed and acceleration achieved by the athlete. Common mistakes occur due to the misconception that athletes must also lean forward, bringing the shoulders ahead of their hands and putting pressure on them. A standard approach to identify sprint start mistakes is to use a stick or weighted string to drop down from the shoulders. The effective implementation of this approach depends on the coach's experience and remains a significant challenge. In this study, a three-dimensional motion capture system with the Vicon® Plug-in-Gait model was used to characterize the kinematic parameters that influence the execution of low-sprint start in six high-performance athletes. The main kinematic parameters are reaction time, stride length, and stride time. The obtained results demonstrate the potential utility of a three-dimensional motion capture system to assess the kinematic parameters of low-sprint start in high-performance athletes.

KEYWORDS: Biomechanics assessment, Kinematic parameters, Low-sprint start

Corresponding author

TO: **Mirvana Elizabeth Gonzalez Macias**

INSTITUTION: **Laboratory Biomechanics, Faculty of Sports, Autonomous University of Baja California**

ADDRESS: **Ave. Monclova S/N, Ex Ejido Coahuila, C. P. 21280, Mexicali, Baja California, México**

CORREO ELECTRÓNICO: **gonzalez.mirvana@uabc.edu.mx**

Received:

21 September 2021

Accepted:

17 February 2022

INTRODUCTION

In the 100 m and 200 m sprint, the success of the sprint start performance depends on the capacity of the athlete to establish a large impulse over the shortest time, reaching the highest running speed as soon as possible [1] [2]. During this step, the sprinters take their positions at the blocks at the set command, and the mechanics of leaving the blocks at the sound of the gun strongly influences the acceleration at the start of a race [3] [4]. When a starter's command is given, the athlete takes up a position with their hands just behind the line, arms vertical, and feet generally placed about a shoe length apart. In the set position, the athlete understands that the hips should rise above the line of the head. The is a misconception that they must lean forward, bringing their shoulders ahead of their hands and putting pressure on them. This position influences the execution of the low-sprint start and can drastically influence the initial running speed and acceleration achieved by the athlete. This is because when the gun goes off, it becomes impossible for the athlete to instantly drive their arms forward or backward without first lifting them off the ground, and they can lose time in the process [5]. According to Schot PK and Knutzen KM, an efficient sprint start depends on the start block positioning and joint angles of the lower limbs in the position [6]. In addition, the pushing time on the blocks and the forces generated by the front and rear legs during the pushing phase depend on the reaction time, stride length, and stride time [7]. The average external power calculated based on horizontal motion and normalized to participant characteristics, provides a single measure that accounts for the change in velocity and the time taken to achieve this change [2]. However, this parameter is more commonly adopted for measurements during early and mid-acceleration after the low-sprint start process.

In practice, an efficient sprint start integrates temporal and spatial acyclic movements into a cyclic action, whose success depends on the athlete's ability and coach experience and is still a big challenge. Different authors have reported studies related to the optimal relationship between body position and initial acceleration. For example, Coh *et al*. reported the dependence of the angular velocity and maximal force of the sprinter during the start on the body positioning and associated start block settings [7]. Mero *et al*. found that block velocity is strongly correlated with the horizontal and vertical forces exerted on the front and rear starting blocks [8]. Gutierrez-Davila, and Prampero *et al*. reported biomechanical variables and their interdependencies with specific motor abilities, energy processes, anthropometric characteristics, and the central processes of motor regulation [9]. There are few previous, reports on the biomechanics of kinematic parameters such as reaction time, stride length, and stride time. All authors state that "a single optimal set position" for all athletes is not recommended because of varying physical factors; therefore, athletes must find their preferred distance between the blocks according to sensations or outcomes.

On the other hand, different technologies have been used to assess the kinematic parameters of sprint start in high-performance athletes. Bezodis *et al*. published in 2019 a clear review of the current biomechanics of track and field sprint starts that can be used to provide current recommendations for both researchers and practitioners [10]. Bezodis *et al*. proposed the use of a laser distance measurement (LDM) device to determine the measurement error in velocity data obtained during different phases of a maximal sprint, and consequently, to evaluate the usability of LDM devices to analyze the velocity profiles of sprinters [11]. Their results recommend that laser data should not be used during the first 5 m of a sprint and are likely to have limited use for assessing within-subject variation in performance during a single session. Bergamini *et al*. reported the use of a lower trunk-mounted inertial measurement unit (IMU) to identify consistent features in the waveforms of the signals

supplied by the IMU and estimate stance and stride duration during the maintenance phase of sprint running. Their results proved that the IMU is suitable for estimating stance and stride durations during sprint running, providing the opportunity to collect information in the field without constraining or limiting athletes' and coaches' activities [12]. Falbriard *et al*. reported the use of foot-worn inertial sensors to investigate different algorithms to detect initial contact (IC) and terminal contact (TC) from different features measured by foot-worn IMU kinematic signals and estimated the main inner-stride temporal parameters. The performance metrics (bias and precision) of each algorithm were assessed in comparison with a reference system (instrumented force plate treadmill), which allowed the validation of the inner-stride temporal parameters over a large number of steps and a large range of running speeds. Their results showed that running speed can significantly affect the estimation bias, suggesting that speed-dependent correction should be applied to improve the accuracy of the systems [13]. Seidl *et al*. reported the use of a radio-based local position measurement system, RedFIR (Grün *et al*., 2011) to obtain spatio-temporal information during sprinting based on lightweight transmitters attached to the athletes. Based on their results, a methodology capable of automatically providing step length, step time, and ground contact time during sprinting was developed. Different transmitter positions were tested, and the accuracy of the derived spatiotemporal parameters was evaluated by comparing them to those from an optoelectronic system [14]. Nagahara *et al*. reported the use of two different global positioning system (GPS) units to obtain mechanical properties during sprint acceleration [15]. However, in their results, they remarked that for the current state of GPS devices' accuracy for speed-time measurements over a maximal sprint acceleration, it is recommended that radar, laser devices, and timing gates remain the reference methods for implementing the computation methods reported by Samozino *et al*. [16]. Bergamini *et al*. validated an adapted sensor-fusion algorithm in a trunk-mounted IMU to estimate trunk inclination and angular velocity during sprint start. A Bland-Altman analysis was carried out using parameters extracted from the historical data of the estimated variables, and analysis of similar curves. Their results indicate agreement between the reference and IMU estimates, which opens a promising scenario for accurate in-field use of IMUs for sprint start performance assessment [17]. Di-Kiat *et al*. proposed the use of an optical motion capture system as a benchmark to validate a new approach for defining running gait. They presented a new gait event identification method, that uses foot acceleration to determine the foot-stroke (FS) and foot-off (FO) times. Temporal parameters such, as contact time and flight time can then be derived from this information [18]. This study also aimed to demonstrate that spatial parameters, such as running speed and stride length, can be estimated accurately using the method presented in [19]. However, most of the technologies described above are only applicable to one athlete, limited to straight runs, and need to be placed directly on the running track. This prohibits their use in competitions and runs including curved sections. Emergency three-dimensional (3D) kinematic analysis computer vision systems use hardware/software processing units with real-time optoelectronic video cameras to measure and quantitatively analyze 3D human segmental movement [20] [21]. Retro-reflective markers placed on the body surface are used to calculate with high precision of the body segments as well as the kinematic joints [22] [23]. The data obtained from these systems are clear and detailed, and the user is able to move freely because there are no cables attached to the computer. In addition, this allows movements in a large volume and observations of more users at one time [22] [23]. The major problem with these systems is the interference. Sometimes, the light reflected from a specific marker has insufficient intensity, which causes inaccuracy in the output. In

addition, the user can sometimes cover the markers, producing an occlusion effect on the camera, which causes inaccuracy of the output. Moreover, the system can be expensive depending on the required sensors, cameras, and software [24].

Although, most kinematic parameters can be obtained from measurements with floor sensors in combination with wearable sensors, no real-time calculations and visualization of 3D segmental movements can be performed. Hence, the aim of this study was to use the Vicon Plug-in-Gait model (Vicon®, Oxford, UK) to characterize the kinematic parameters that influence the execution of low-sprint start in six high-performance athletes [25]. The main kinematic parameters are reaction time, stride length, and stride time. Average external power was not considered in this study because vertical movement and vertical velocity play an important role in the low sprint-start process. The obtained results demonstrate the potential utility of the system in assessing the kinematic parameters of a low-sprint start.

MATERIALS AND METHODS

Participants

Six high-performance athletes, three women, and three men, who compete in 100 meters passing hurdles, were evaluated. All athletes wore tight training shorts, and the women wore a sports female bra. During testing, athletes wore the footwear that they used for competition. No accessories that hindered or introduced variations in athlete performance were permitted during testing. The demographic data (age, height, body mass) are as follows: (mean ±SD, age = 17 ± 2.09 years); the height of the athletes was measured with a wall stadiometer graduated in centimetres, presenting a scale from 0 to 250cm(SECA), without shoes, straight back, front view, (Height = 1.69 ± 0.06 m) and the body mass was obtained using the AMTI platform, (Body mass = 59.77 ± 6.65 kg).

Anthropometric dimensions were measured according to the provisions of the Vicon® Plug-in Gait product guide [25] as shown in Table 1. Flexible tape and Vernier tape were used for measurements. This study conformed to the recommendations of the Declaration of Helsinki and was approved by the research and postgraduate ethics and evaluation committee of the Faculty of Sports of the Autonomous University of Baja California, México.

TABLE 1. The averages of the anthropometric and demographic measures of the participants.

Variable	Male	Female
Age (years)	16 ± 1	18 ± 2.64
Height (m)	1.73 ± 0.02	1.66 ± 0.07
Body mass (kg)	61.56 ±3.17	57.97 ± 9.52
LPI (cm)	90.6 ± 6.03	86.53 ± 5.85
LPD (cm)	89.66 ± 5.57	86.76 ± 5.56
DRI (cm)	9.56 ± 0.47	8.6 ± 0.34
DRD (cm)	9.46 ± 0.55	8.63 ± 0.35
DTI (cm)	6.73 ± 0.35	6.7 ± 0.36
DTD (cm)	6.76 ± 0.46	6.86 ± 0.45
DHI (cm)	6.7 ± 0.52	5.26 ± 0.30
DHD (cm)	5.53 ± 0.57	5.3 ± 0.79
DCI (cm)	6.73 ± 0.057	5.76 ± 0.20
DCD (cm)	6.9 ± 0.10	5.96 ± 0.15
DMI (cm)	5.58 ± 0.27	4.73 ± 0.25
DMD (cm	5.56 ± 0.32	4.76 ± 0.11
EMI (cm)	2.73 ± 0.11	2.16 ± 0.1
EMD (cm)	2.7 ± 0.1	2.1 ± 0.1

LPI = Left Leg Length, LPD = Right Leg Length, DRI = Left Knee Diameter, DRD = Right Knee Diameter, DTI = Left Ankle Diameter, DTD = Right Ankle Diameter, DHI = Left Shoulder Displacement, DHD = Right Shoulder Displacement, DCI = Left Elbow Diameter, DCD = Right Elbow Diameter, DMI = Left Wrist Diameter, DMD = Right Wrist Diameter, EMI = Left hand Thickness, EMD = Right Hand Thickness.

Marker placement and Motion Capture

The evaluations were performed at the Biomechanics Laboratory of the Faculty of Sports at the Autonomous University of Baja California, Mexico. 39 passive reflective markers, 24 mm in diameter, were placed on each

participant as shown in Figure 1. The position of each reflective marker followed the standard Plug-in-Gait model, as described in Table 2. To characterize complete body movement, the markers were divided into upper-body and lower-body markers. The upper body markers contained four head markers, two for the front side and two for the backside. The torso markers contained five markers, two for vertebrae, a clavicle marker, a sternum marker and a scapula marker. The arm markers contain a marker for the shoulder and, markers for the upper arms, elbow, forearm, wrist, and fingers. Similarly, the lower body markers contained five pelvis markers, two for the left anterior superior side and two for the right anterior superior side of the iliac spine. The leg contained five markers, a knee marker, thigh marker, ankle marker, and tibial marker. The foot contained a toe and heel marker.

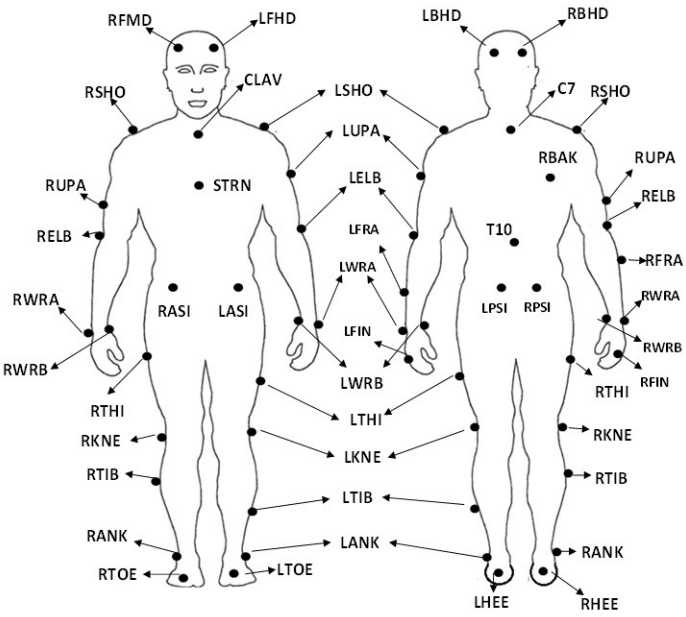

FIGURE 1. Skeleton model illustrating the placement of the passive reflective markers (anterior and posterior view).

The three-dimensional motion capture system used contained eleven optoelectronics infrared cameras (Bonita B10) up to one megapixel (1024 x 1024) high resolution, which accurately captures up to 0. 5 mm for a 4 m x 4 m volume, with variable focal length, and speed of 250 frame rate (fps), and two video cameras (Bonita 720c) of a 1280 x 720 HD resolution, with an impressive 120 Hz fully synchronized frame rate. The cameras were distributed in the capture volume to measure all possible details in the athlete's movement in 3D. In addition, the system includes a Giganet camera switch (POE) in an Ethernet network, a Vicon lock for analog signal observation, a host PC with Vicon Nexus 2 software, and two force platforms at 1000 Hz (AMTI, Waterdown, MA, USA). Figure 2 illustrates the setup of the capture system. In addition, all demographic and anthropometric dimensions of the participants were captured using the Nexus 2 software.

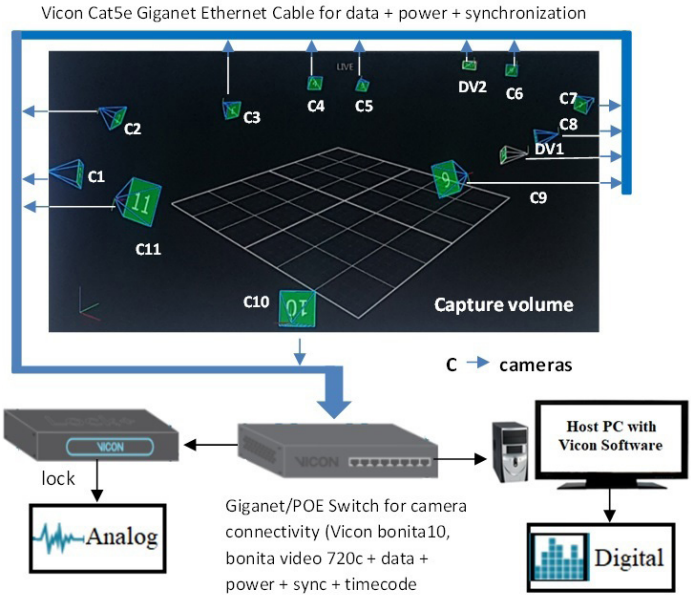

FIGURE 2. Set-up of the athlete movement captures system.

Figure 3 shows a general diagram of the Vicon Nexus 2 system. Before starting the test, it was necessary to calibrate the video and infrared cameras using the T-rod tool. The T-rod tool carries five LEDs, and this tool moves at the area work of 6 x 4m. Is was then necessary to place this at the origin point on the floor, according to the method described [25] in Figure 3(a).

TABLE 2. Plug-in-Gait model, markers placement.

Upper Body		
	Head Markers	
LFHD	Left front head	Located approximately over the left template
RFHD	Right front head	Located approximately over the right template
LBHD	Left-back head	Placed on the back of the head
RBHD	Right-back head	Placed on the back of the head
	Torso Markers	
C7	7th Cervical Vertebrae	Spinous process of the 7th cervical vertebrae
T10	10th Thoracic Vertebrae	Spinous process of the 10th thoracic vertebrae
CLAV	Clavicle	Jugular Notch where the clavicles meet the sternum
STRN	Sternum	Xiphoid process of the Sternum
RBAK	Right Back	Placed in the middle of the right scapula
	Arms Markers	
LSHO	Left shoulder marker	Placed on the Acromio-clavicular joint
LUPA	Left upper arm marker	Placed on the upper arm
LELB	Left elbow	Placed on the lateral epicondyle
LFRA	Left forearm marker	Placed on the lower arm
LWRA	Left wrist marker A	Left wrist bar thumb side
LWRB	Left wrist marker B	Left wrist bar pinkie side
LFIN	Left fingers	Placed on the dorsum of the hand
RSHO	Right shoulder marker	Placed on the Acromio-clavicular joint
RUPA	Right upper arm marker	On the lateral area in the lower third of the arm
RELB	Right elbow	On the lateral epicondyle
RFRA	Right forearm marker	On the lateral area in the upper third of the forearm
RWRA	Right wrist marker A	Next to the thumb on the wrist
RWRB	Right wrist marker B	Next to the pinky on the wrist
RFIN	Right fingers	Placed on the dorsum of the hand
Lower Body		
	Pelvis	
LASI	Left ASIS	Placed directly over the left anterior superior iliac spine
RASI	Right ASIS	Placed directly over the right anterior superior iliac spine
LPSI	Left PSIS	Placed directly over the left posterior superior iliac spine
RPSI	Right PSIS	Placed directly over the right posterior superior iliac spine
	Leg Markers	
LKNE	Left knee	Placed on the lateral epicondyle of the left knee
LTHI	Left thigh	Placed over the lower lateral 1/3 surface of the thigh
LANK	Left ankle	Placed on the lateral malleolus along an imaginary line that passes through the transmalleolar axis.
LTIB	Left tibial wand marker	Similar to the thigh markers, these are placed over the lower 1/3 of the shank to determine the alignment of the ankle flexion axis
RKNE	Right knee	Placed on the lateral epicondyle of the right knee
RTHI	Right thigh	Placed on the upper lateral 1/3 surface of the thigh
RANK	Right ankle	Placed on the lateral malleolus along an imaginary line that passes through the transmalleolar axis.
RTIB	Right tibial wand marker	Placed on the upper 1/3 of the lateral surface of the stem
	Foot Markers	
LTOE	Left toe	Placed over the second metatarsal head, on the mid-foot side of the equinus break between fore-foot and mid-foot
LHEE	Left heel	Placed on the calcaneous at the same height above the plantar surface of the foot as the toe marker
RTOE	Right toe	Placed over the second metatarsal head, on the mid-foot side of the equinus break between fore-foot and mid-foot
RHEE	Right heel	Placed on the calcaneous at the same height above the plantar surface of the foot as the toe marker

When the markers were placed, the athlete was notified to enter into a static position, as shown in Figure 3(b), to perform static capture. The system then detected the markers, as shown in Figure 3(c), and performed the reconstruction model, as shown in Figure 3(d). Once the reconstruction model was obtained, the athlete performed the movement, and the trajectories of the markers were labeled and filtered using a Butterworth low-pass filter with a frequency of 100Hz.

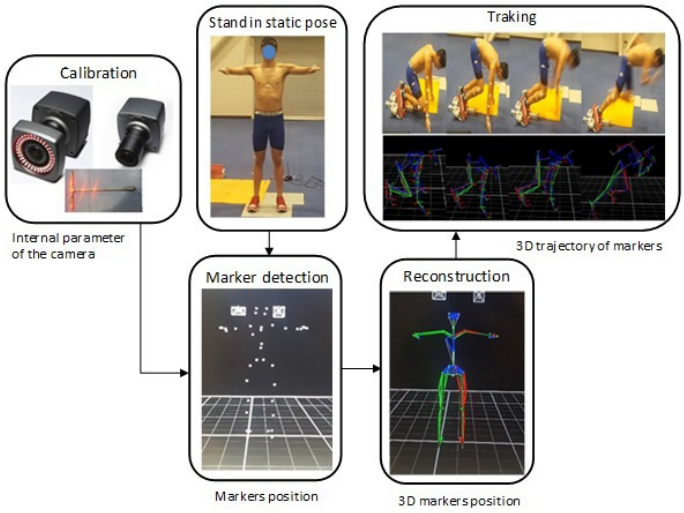

FIGURE 3. The general operation of the system. (a) Calibration of the cameras (b) athlete static starting position (c) markers detectio (d) Reconstruction 3D markers.

Description of the applied exercise

In this study, the reaction time (RT) is defined as the time between the sound emitted by the timing system and the time the foot of the athlete leaves the starting block. The wireless Brower Timing Systems TS-T17 was used to measure the RT. To avoid the risk of injury and achieve maximum performance, the athletes realized a standardized dynamic warm-up before the tests. To capture the movement of the athletes during the start of running three critical steps were performed. The first step is positioning the athlete at the starting block. Once the athlete is placed in the correct position, the athlete hears the first beep emitted by the Brower Timing Systems, which means being prepared. The second step is when a second beep is emitted, which indicates being ready for the athlete, and the third step is when a third beep is emitted and the start is executed, as shown in Figure 4. Once the start is executed, the RT is obtained, the first impact of the reaction force from the ground in three steps 1) moment of release of the foot from the block, 2) maximum extension of the leg behind and 3) the first contact of the foot with the ground. At that moment, the stride length and stride time were determined by the motion capture system.

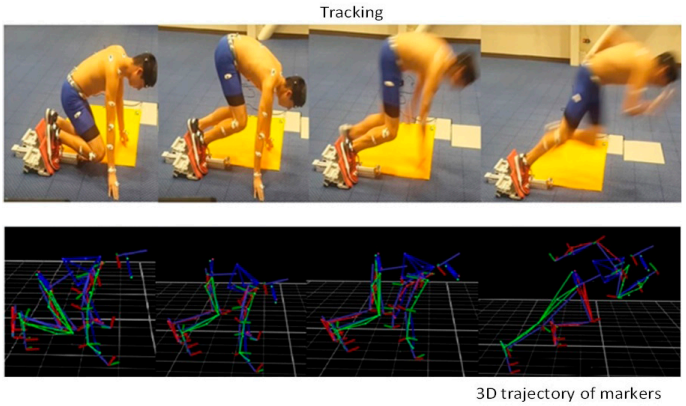

FIGURE 4. The capture of 3D trajectory of markers in the system.

Data processing

The 3D trajectories of the passive reflective markers were corrected using a low pass filter (100Hz Butterworth filter) and then imported into Matlab R2019b (The MathWorks, Inc).

Stride length

Stride length is the distance from the point where the toe leaves the starting block until it touches the ground again (after the swing phase). The TOE marker was used to calculate stride length using equation (1) [26].

$$L = \sqrt{(X_{end} - X_{start})^2 + (Y_{end} - Y_{start})^2 + (Z_{end} - Z_{start})^2} \quad (1)$$

where L is the stride length.

Stride time

Stride time was calculated using the total number of frames and the elapsed time between frames. The square where the foot takes off is considered to be the square with which it first impacts the ground. In this case, the time between frames is 0.01 s. Therefore, it was calculated using equation (2) as follows [26].

$$T = (0.01 \times N_F) \quad (2)$$

Where T is the stride time and NF is the number of frames.

Statistical analysis

R software was used for statistical analysis [27]. Descriptive statistics (mean ± SD) were determined for each variable. The Shapiro-Wilk test was applied because the sample size was less than fifty which complies with the normal principle (p> 0.05). In this sense, the parametric test was used, the Student's t-test was used for independent samples.

RESULTS AND DISCUSSION

Table 3 shows the results of the three variables evaluated in men. In this group, M1 obtained the shortest reaction time of 0.19 s and a stride length of 1.36 m with the right leg behind, while with the left leg behind, which is the leg that normally performs the

TABLE 3. Obtained results of the 3 evaluated variables for male.

Participant	Reaction time (LLB)	Stride length (m)	Stride time (S)	Reaction time (RLB)	Stride right (m)	Stride time (S)
M1	0.32	1.357	0.34	0.19	1.369	0.36
M1	0.32	1.120	0.34	0.19	1.130	0.36
M1	0.35	1.070	0.37	0.20	1.140	0.38
M2	0.28	0.950	0.28	0.30	1.074	0.30
M2	0.30	1.020	0.32	0.32	1.070	0.30
M2	0.28	0.950	0.29	0.31	1.100	0.34
M3	0.23	1.227	0.31	0.28	1.264	0.28
M3	0.23	1.120	0.30	0.28	1.020	0.27
M3	0.25	1.100	0.30	0.30	1.120	0.30

TABLE 4. Obtained results of the 3 evaluated variables for female.

Participant	Reaction time (LLB)	Stride length (m)	Stride time (S)	Reaction time (RLB)	Stride right (m)	Stride time (S)
F1	0.34	1.010	0.32	0.32	0.870	0.30
F1	0.36	1.100	0.35	0.35	1.010	0.30
F1	0.24	1.110	0.32	0.32	1.047	0.31
F2	0.25	1.115	0.28	0.28	1.106	0.32
F2	0.25	1.110	0.27	0.27	1.010	0.33
F2	0.25	0.980	0.28	0.28	1.080	0.33
F3	0.25	1.100	0.34	0.27	1.010	0.33
F3	0.25	1.200	0.34	0.26	1.288	0.31
F3	0.25	0.980	0.33	0.26	1.080	0.30

start; he obtained the longest reaction time of 0.32s. Besides, the group of men obtained a mean of 0.276 with a standard deviation of 0.04 in reaction time using the left leg behind while a mean of 0.256 with a standard deviation of 0.05 in reaction time was obtained with the right leg behind. Similarly, Table 4 shows the results of the 3 variables evaluated in women. In this group, F1 obtained the best reaction time of 0.24s and a stride length of 1.11 m with the left leg behind, while with the left leg behind, which is not the leg that normally performs the start, she obtained the longest reaction time of 0.32s. In addition, the group of women obtained a mean of 0.28 with a standard deviation of 0.05 in reaction time using the left leg behind while a mean of 0.263 with a standard deviation of 0.03 in reaction time was obtained using the right leg behind. From Tables 3 and 4, it is observed that men performed better in reaction times, as well as greater stride length, than to women. Table 5 presents the descriptive statistics of each variable evaluated in men and women.

TABLE 5. Descriptive statistics for each variable evaluated.

Variable	Participants	Mean	SD
Reaction Time (LLB)	Male	.28	.046
	Female	.27	.036
Stride length (m)	Male	1.10	.112
	Female	1.07	.013
Stride time (S)	Male	.31	.029
	Female	.31	.032
Reaction time (RLB)	Male	.26	.061
	Female	.29	.035
Stride right (m)	Male	1.14	.066
	Female	1.05	.075
Stride time (S)	Male	0.32	0.42
	Female	0.31	0.12

The Student's t-test for independent samples indicates that Ho is acceptable, that is, there are no significant differences between men and women.

Table 6 shows the results obtained from the Student´s T-test, degrees of freedom, and p-values >0.05.

TABLE 6. Independent samples of Student´s t-test results.

Variable	t	gl	*p*
Reaction Time (LLB)	.401	4	.709
Stride length (m)	.357	4	.739
Stride time (S)	.079	4	.941
Reaction time (RLB)	-.647	4	.553
Stride right (m)	1.506	4	.207
Stride time (S)	.261	4	.807

Figure 5 shows the left toe speed obtained for the male and female participants. It is observed that all participants reached their highest left toe speed between 13 and 20 s. It is also observed that male participants (M2) reached the highest speed of 7.5 m/s at 16s while the female participants (F3) reached the lowest speed of 7.1 m/s at 18 s.

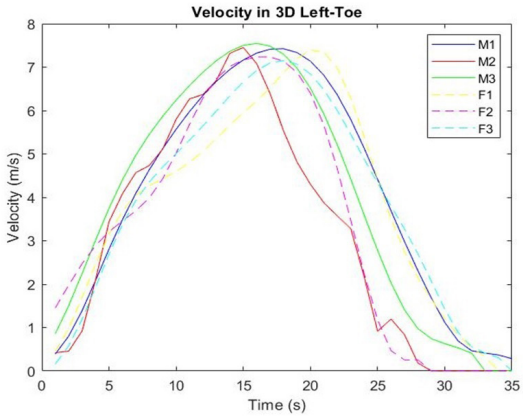

FIGURE 5. Speed obtained for male and female participants on the left-toe.

Similarly, Figure 6 shows the right-toe speed obtained for male and female participants.

It is observed that the participants reached the highest speed on the right toe between 15 and 25 s. It is also observed that male (M2) reached the highest speed of

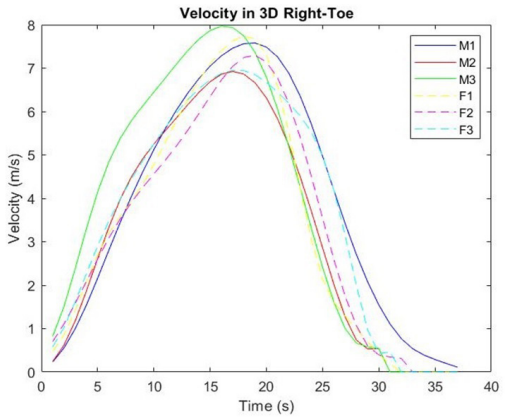

FIGURE 6. **Speeds were obtained for male and female participants on the right-toe.**

7.96 m/s at 16 s while the male (M1) reached the lowest speed of 6.9 m/s at 17 s. Besides, the female participant (F3) obtained the lowest speed of 6.9 m/s at 17 s while the participant (F1) obtained the maximum speed of 7.7 m/s at 18 s. From Figure 5 and Figure 6 it is observed that the best speeds are obtained on the right toe, which is in contrast with the common practice that indicates the left toe behind is the toe that participants normally perform the start.

In this study, the Helen-Hayes PGM for snatch output motion analysis was used to determine the reaction time, stride length, and stride time of both legs of the six athletes. The Vicon® Plug-in-Gait model (PGM) is one of the most widely used models for evaluating different kinematic and kinetic parameters of different motor or sports gestures [28] [29] [30]. Remi K. reported that stride length, determined when the rear leg moves forward in the frontal plane, ranges from 100 to 120 cm [31]. Considering this range, in the group of men, (M2) in two of the three repetitions of the left leg behind, obtained 0.950 m, while with the right leg behind, all values were within the range. In the group of women (F2) and (F3) with the left leg behind in the last repetition did not obtain (100-120cm). With respect to the right leg behind (F1) was the only one, where the value was not within the reported Remi K. range.

Slawinski J *et al*. used an optoelectronic motion analysis system containing 12 digital cameras (250 Hz) to characterize four repetitions of sprint snatches of six elite sprinters and six well-trained sprinters. The average RT of the elite sprinters was 0.151 ± 0.016 s, and that of the six well-trained sprinters was 0.158 ± 0.033 s [32].

In comparison with the results obtained by Slawinski J *et al*., the sprinters characterized in this study obtained a higher performance. For three repetitions, they obtained an average RT of 0.2767 ± 0.045 s using the right leg back, and an average RT of 0.2778 ± 0.042 s using the left leg back. There is a difference in their RT averages, however, it is not significant considering that they are elite and well-trained sprinters. Despite the small sample size, this study aimed to characterize the snatch output, using a motion analysis system, and make pertinent corrections to obtain the RT, stride length, and stride time for each leg of the athletes.

CONCLUSIONS

In this study, a 3D motion capture system was used to characterize the kinematic parameters that influence the execution of a low-sprint start in high-performance athletes. The Vicon 3D capture system is precise and highly accurate for performing biomechanical evaluations of body motor gestures. The high reliability obtained data is not just empirical, but also numerical ones. Although a small number of samples were used, the results provide evidence of the effectiveness of using 3D capture technology to quantify kinematic parameters of low-sprint starts. The characterized kinematic parameters can be used to identify improvements for the athlete, such as errors in the execution of the start to avoid possible injuries in the athlete. The Student's t-test for independent samples indicates that Ho is accepted, and there are no significant differences between men and women (p-value > 0.05), for all the variables. However, with this technology, it was found that three athletes obtained better times with the nondominant leg. In addition, this study illustrated the importance of

coaches and the athletes understanding of the use of 3D motion capture system technology and its scope. This technology can be part of their evaluations to avoid possible injuries, detect errors in the execution of precision movements, and improve performance.

ETHICAL STATEMENT

The present study followed the ethical principles regarding human experimentation proposed by the Helsinki declaration; all the subjects provided a written consent in order to participate in the study, that was approved by the research and postgraduate ethics and evaluation committee of the Faculty of Sports of the Autonomous University of Baja California, México. Protocol #149/2569.

AUTHOR CONTRIBUTIONS

M.E.G.M performed data curation, designed, and developed methodology, applied techniques to analyze or synthesize data, validated and tested the models employed, oversaw implementation of software for biomechanical analysis, elaborated images, carried out statistical analysis, provided material and computer resources, and participated in all the writing stages of the manuscript. C.V.A oversaw the development of the methodology, validated the models employed, participated in the writing of the manuscript, and reviewed and edited the final version. E.M.A.M performed data curation, analyzed data, and implemented software for data analysis. K.R.K.G. performed data curation and implemented software for data analysis. All authors conceptualized the project, reviewed and approved the final version of the manuscript.

ACKNOWLEDGMENTS

The author would like to thank to the Sport and Culture Institute (INDE) of the state of Baja California, México and the Sports Faculty of the Autonomous University of Baha California for allowing the use of equipment and facilities for the development of the present study.

CONFLICTS OF INTEREST

The authors do not report any conflict of interest.

REFERENCES

[1] Fortier S, Basset FA, Mbourou G, Favérial J, Teasdale N. Starting block performance in sprinters: A statistical method for identifying discriminative parameters of the performance and an analysis of the effect of providing feedback over a 6-week period. J Sport Sci Med [Internet]. 2005;4(2):134-143. Available from: *https://www.jssm.org/jssm-04-134.xml%3EFulltext#*

[2] Bezodis NE, Salo AI, Trewartha G. Choice of sprint start performance measure affects the performance-based ranking within a group of sprinters: Which is the most appropriate measure? Sports Biomech [Internet]. 2010;9(4):258-269. Available from: https://doi.org/10.1080/14763141.2010.538713

[3] Guissard N, Duchateau J, Hainaut K.. EMG and mechanical changes during sprint starts at different front block obliquities. Med Sci Sports Exerc [Internet]. 1992;24(11):1257-1263. Available from: *https://journals.lww.com/acsm-msse/Abstract/1992/11000/EMG%20and%20mechanical%20changes%20during%20sprint%20starts%20at.10.aspx*

[4] Slawinski J, Dumas R, Cheze L, Ontanon G, et al. 3D Kinematic of Bunched, Medium and Elongated Sprint Start. Int J Sports Med [Internet]. 2012;33(7):555-560. Available from: https://doi.org/10.1055/s-0032-1304587

[5] Theophilos P, Nikolaos M, Kiriakos A, Athanasia S, et al. Evaluation of sprinting performance in adolescent athletes with running shoes, spikes and barefoot. J Phys Educ Sport [Internet]. 2014;14(4):593-598. Available from: http://dx.doi.org/10.7752/jpes.2014.04092

[6] Schot PK, Knutzen KM. A Biomechanical Analysis of Four Sprint Start Positions. Res Q Exerc Sport [Internet]. 1992;63(2):137-147. Available from: https://doi.org/10.1080/02701367.1992.10607573

[7] Čoh M, Peharec S, Bačić P, Mackala K. Biomechanical Differences in the Sprint Start between Faster and Slower High-Level Sprinters. J Hum Kinet [Internet]. 2017;56(1):29-38. Available from: https://dx.doi.org/10.1515%2Fhukin-2017-0020

[8] Mero A, Komi PV, Gregor RJ. Biomechanics of Sprint Running. Sports Med [Internet]. 1992;13(6):376-392. Available from: https://doi.org/10.2165/00007256-199213060-00002

[9] Gutiérrez-Dávila M, Dapena J, Campos J. The Effect of Muscular Pre-Tensing on the Sprint Start. J Appl Biomech [Internet]. 2006;22(3):194-201. Available from: https://doi.org/10.1123/jab.22.3.194

[10] Bezodis NE, Willwacher S, Salo AIT. The Biomechanics of the Track and Field Sprint Start: A Narrative Review. Sports Med [Internet]. 2019;49(9):1345-1364. Available from: https://doi.org/10.1007/s40279-019-01138-1

[11] Bezodis NE, Salo AIT, Trewartha G. Measurement Error in Estimates of Sprint Velocity from a Laser Displacemeny Measurement Device. Int J Med [Internet]. 2012;33(6):439-444. Available from: https://doi.org/10.1055/s-0031-1301313

[12] Bergamini P, Picerno P, Pillet H, Natta F, et al. Estimation of temporal parameters during sprint running using a trunk-mounted inertial measurement unit. J Biomech [Internet]. 2012;45(6):1123-1126. Available from: https://doi.org/10.1016/j.jbiomech.2011.12.020

[13] Falbriard M, Meyer F, Mariani B, Millet GP, et al. Accurate Estimation of Running Temporal Parameters Using Foot-Worn Inertial Sensors. Front Physiol [Internet]. 2018;9:610. Available from: https://dx.doi.org/10.3389%2Ffphys.2018.00610

[14] Seidl T, Linke D, Lames M. Estimation and validation of spatio-temporal parameters for sprint running using a radio-based tracking system. J Biomech [Internet]. 2017;65:89-95. Available from: https://doi.org/10.1016/j.jbiomech.2017.10.003

[15] Nagahara R, Botter A, Rejc E, Koido M, et al. Concurrent Validity of GPS for Deriving Mechanical Properties of Sprint Acceleration. Int J Sports Physiol Perform [Internet]. 2017;12(1):129-132. Available from: https://doi.org/10.1123/ijspp.2015-0566

[16] Samozino P, Rabita G, Dorel S, Slawinski J, et al. A simple method for measuring power, force, velocity properties, and mechanical effectiveness in sprint running. Scand J Med Sci Sports [Internet]. 2016;26(6):648-658. Available from: https://doi.org/10.1111/sms.12490

[17] Bergamini E, Guillon P, Camomilla V, Pillet H, et al. Trunk Inclination Estimate During the Sprint Start Using an Inertial Measurement Unit: A Validation Study. J Appl Biomech [Internet]. 2013;29(5):622-627. Available from: https://doi.org/10.1123/jab.29.5.622

[18] Chew D-K, Ngoh KJH, Gouwanda D, Gopalai AA. Estimating running spatial and temporal parameters using an inertial sensor. Sports Eng [Internet]. 2018;21:115-122. Available from: https://doi.org/10.1007/s12283-017-0255-9

[19] Yang S, Mohr C, Li Q. Ambulatory running speed estimation using an inertial sensor. Gait Posture [Internet]. 2011;34(4):462-466. Available from: https://doi.org/10.1016/j.gaitpost.2011.06.019

[20] Savoie P, Cameron JAD, Kaye ME, Scheme EJ. Automation of the Timed-Up-and-Go Test Using a Conventional Video Camera. IEEE J Biomed Health Inform [Internet]. 2020;24(4):1196-205. Available from: https://doi.org/10.1109/jbhi.2019.2934342

[21] Thomas G, Gade R, Moeslund TB, Carr P, et al. Computer vision for sports: Current applications and research topics. Comput Vis Image Underst [Internet]. 2017;159:3-18. Available from: https://doi.org/10.1016/j.cviu.2017.04.011

[22] Begon M, Colloud F, Fohanno V, Bahuaud P, et al. Computation of the 3D kinematics in a global frame over a 40 m-long pathway using a rolling motion analysis system. J Biomech [Internet]. 2009;42(16):2649-2653. Available from: 10.1016/j.jbiomech.2009.08.020

[23] Bernardina GRD, Monnet T, Pinto HT, de Barros RML, et al. Are Action Sport Cameras Accurate Enough for 3D Motion Analysis? A Comparison With a Commercial Motion Capture System. J Appl Biomech [Internet]. 2019;35(1):80-86. Available from: https://doi.org/10.1123/jab.2017-0101

[24] Guerra-Filho G. Optical Motion Capture: Theory and Implementation. Theor App Inform. 2005;12:61-90.

[25] Vicon. Plug-In Gait modelling instructions. Vicon® Manual, Vicon® Motion Systems [Internet]. Oxford Metrics Ltd; 2002. Available from: *https://www.vicon.com/software/oxford-foot-model/*

[26] Arellano-González JC, Medellin-Castillo HI, Cardenas-Galindo JA. Analysis of the kinematic variation of human gait under different walking conditions using computer vision. Rev Mex Ing Biomed [Internet]. 2017;38(2):437-457. Available from: https://doi.org/10.17488/rmib.38.2.2

[27] GNU. The R Project for Statistical Computing [Internet]. R;2016. Available from: *https://www.R-project.org/*

[28] Nair SP, Gibbs S, Arnold G, Abboud R, et al. A method to calculate the centre of the ankle joint: A comparison with the Vicon® Plug-in-Gait model. Clin Biomech [Internet]. 2010;25(6):582-587. Available from: https://doi.org/10.1016/j.clinbiomech.2010.03.004

[29] Khamis S, Danino B, Springer S, Ovadia D, et al. Detecting Anatomical Leg Length Discrepancy Using the Plug-in-Gait Model. Appl Sci [Internet]. 2017;7(9):926. Available from: https://doi.org/10.3390/app7090926

[30] Duffell LD, Hope N, McGregor AH. Comparison of kinematic and kinetic parameters calculated using a clusterbased model and Vicon's plug-in gait. Proc Inst Mech Eng H [Internet]. 2014;228(2):206-210. Available from: https://doi.org/10.1177/0954411913518747

[31] Korchemny R. A new concept for sprint start and acceleration training. New Stud Athl [Internet]. 1992;7(4):65-72. Available from: *http://centrostudilombardia.com/wp-content/uploads/IAAF-Corsa-Velocita/1992-A-new-concept-for-sprint-start-and-acceleration-training.pdf*

[32] Slawinski J, Bonnefoy A, Levêque J-M, Ontanon G, et al. Kinematic and Kinetic Comparisons of Elite and Well-Trained Sprinters During Sprint Start. J Strength Cond Res [Internet]. 2010;24(4):896-905. Available from: https://doi.org/10.1519/jsc.0b013e3181ad3448